Liquid Crystals
Publication details, including instructions for authors and subscription information:
http://www.informaworld.com/smpp/title~content=t713926090

X-ray investigations on the cyclopalladated mesogen bis-{5-(1-nonyl)-2{[4'1-nonyloxy)phenyl-2'-ato]}pyrimidine-N',C$^{2'}$]-μ-iodo}dipalladium(II)

Mauro Ghedini[a]; Daniela Pucci[a]; Roberto Bartolino[b]; Oriano Francescangeli[c]
[a] Dipartimento di Chimica, Università della Calabria, Arcavacata (CS), Italy [b] Dipartimento di Fisica, Università della Calabria, Arcavacata (CS), Italy [c] Dipartimento di Scienze dei Materiali e della Terra, Sezione Fisica, Università di Ancona, Ancona, Italy

To cite this Article Ghedini, Mauro , Pucci, Daniela , Bartolino, Roberto and Francescangeli, Oriano(1993) 'X-ray investigations on the cyclopalladated mesogen bis-{5-(1-nonyl)-2{[4'1-nonyloxy)phenyl-2'-ato]}pyrimidine-N',C$^{2'}$]-μ-iodo}dipalladium(II)', Liquid Crystals, 13: 2, 255 — 263
To link to this Article: DOI: 10.1080/02678299308026299
URL: http://dx.doi.org/10.1080/02678299308026299

LIQUID CRYSTALS, 1993, VOL. 13, NO. 2, 255–263

X-ray investigations on the cyclopalladated mesogen bis-{5-(1-nonyl)-2{[4′(1-nonyloxy)phenyl-2′-ato]}pyrimidine-N′,C$^{2'}$]-μ-iodo}dipalladium(II)

by MAURO GHEDINI*, DANIELA PUCCI
Dipartimento di Chimica, Università della Calabria,
I 87036 Arcavacata (CS), Italy

ROBERTO BARTOLINO
Dipartimento di Fisica, Università della Calabria,
I 87036 Arcavacata (CS), Italy

and ORIANO FRANCESCANGELI
Dipartimento di Scienze dei Materiali e della Terra,
Sezione Fisica, Università di Ancona,
Via Brecce Bianche, I-60131 Ancona, Italy

(*Received 25 May 1992; accepted 15 September 1992*)

The cyclopalladated complex $[Pd(L_3)(\mu\text{-}I)]_2$ ($[Pd(L_3)(\mu\text{-}I)]_2$ = bis-{5-(1-nonyl)-2{[4′(1-nonyloxy)phenyl-2′-ato]}pyrimidine-N′,C$^{2'}$]-μ-iodo}dipalladium (II); C→105·1°C (C_1)→128·1°C (S_A)→202·5°C (I)) has been investigated by X-ray diffraction and the electron density profile along the director, in the smectic phase, determined. $[Pd(L_3)(\mu\text{-}I)]_2$ is a mesogenic species with a lateral–lateral fused molecular shape whose main features are: (i) the solid C_1 phase when observed with a polarizing microscope gives a polygonal texture like a smectic A phase, and (ii) to describe properly the electron density profile along the director a model which takes into account a high electron density area (i.e. the four aromatic rings and the Pd_2I_2 fragment) extending perpendicular to the director is required.

1. Introduction

Within the studies focused to the preparation of metallo-mesogens, several cyclopalladated compounds which display thermotropic properties have been reported [1–5]. Among them, we recently reported the organometallic complexes $[Pd(L_n)(\mu\text{-}X)]_2$ (X = Cl, Br, I) arising from a series of liquid-crystalline ligands HL_n containing the 2-phenylpyrimidine skeleton [2]. The molecular structure of this species (see figure 1) consists of two ligands, in a *transoid* geometry with respect to the Pd---Pd axis, connected by the Pd_2X_2 bridge. Thus, comparing the uncomplexed ligands with their palladium derivatives, shows that complexation enlarges the rigid molecular core.

* Author for correspondence.

0267–8292/93 $10·00

HL_1: $R = C_9H_{19}$; $R' = CH_3$

HL_2: $R = C_6H_{13}$; $R' = C_{11}H_{23}$

HL_3: $R = C_9H_{19}$; $R' = C_9H_{19}$

X = Cl,Br,I

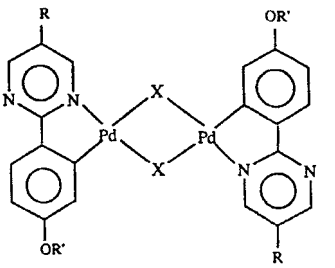

Figure 1. Molecular structure of the cyclopalladated 2-phenylpyrimidine complexes.

Indeed the mesophases become more ordered: for example, nematics for HL_n and smectics for $[Pd(L_n)(\underline{\mu}\text{-}X)]_2$ [2].

The characterization of the textures of smectic phases was previously performed through polarizing microscopy observations. In particular, with reference to the iodinated HL_3 complex, two different polygonal textures, both apparently accounting for S_A phases, were recognized. These mesophases were reported as S_A and S_X, where S_A designated the lowest temperature one [2].

These metallo-mesogens present a lateral–lateral fused molecular shape [6] and X-ray investigations performed on the S_A phases displayed by copper complexes having similar structural features indicate an interdigitated molecular array [7–9]. Thus, in principle several smectic A phases differing in the degree of interdigitation and showing very similar optical textures, cannot be excluded. In order to elucidate this point the two S_A and S_X mesophases detected for the $[Pd(L_3)(\underline{\mu}\text{-I})]_2$ complex have been studied by X-ray diffraction. Here we report the results obtained. On the basis of these results the previous phase identification carried out by means of optical microscopy must be partially modified. In particular, the X-ray diffraction patterns unequivocally indicate that the mesophase previously identified as S_A really is a solid phase C_1 while the mesophase classified as S_X is indeed a smectic A phase.

2. Experimental

The compound bis-{5-(1-nonyl)-2{[4′(1-nonyloxy)phenyl-2′-ato]}pyrimidine-N′,-$C^{2'}$]-μ-iodo}dipalladium(II) has been prepared as reported previously [2]. X-ray diffraction measurements have been performed by using two different X-ray diffractometers. In the first experiment, X-ray diffraction photographs were obtained by a Rigaku-Denky RV300 rotating anode generator equipped with a pin-hole flat camera. The primary beam of Ni-filtered Cu–K_α radiation ($\lambda = 1{\cdot}54$ Å) impinged on the ~ 1 mm thick sample, the temperature of which was controlled to $\pm 0{\cdot}3°$ by a hot stage containing electrical resistors. The optical density of the X-ray diffraction photographs was measured by a conventional microdensitometer. The measurements were subsequently repeated by using the INEL CPS 120 powder diffractometer equipped with a position sensitive detector covering 120° in the scattering angle 2θ, with an angular resolution of 0·018° in θ. Ge(101) monochromatized Cu–K_α radiation, collimated with an appropriate slit system (beam dimensions: 0·5 mm × 8 mm), was used. A calibration compound with well-known 2θ values was used to determine the calibration function which describes the 2θ versus channel number function. The samples, ~ 1 mm thick were placed between two thin aluminium sheets, fixed to a circular hole (1 cm diameter) in an aluminium sample holder. Heating was achieved by a hot stage whose stability

was $\pm 0{\cdot}1$°C. X-ray diffraction spectra were recorded at different temperatures between room temperature and the clearing temperature, both on heating and on cooling.

The integrated intensities of the Bragg reflections from the smectic phase were obtained from the corresponding spectrum after background subtraction and deconvolution for the instrumental resolution function, followed by correction for the Lorentz and polarization factors. In our geometry, the Lorentz factor is [10]

$$L(\theta)=\frac{1}{\sin^2\theta\cos\theta} \tag{1}$$

and the use of the (101) reflection on the Ge monochromator gives a polarization factor [11]

$$P(\theta)=\frac{1+\cos^2 2\alpha\cos^2 2\theta}{1+\cos^2 2\alpha}, \tag{2}$$

with $\alpha=11{\cdot}1°$. The experimental results have, therefore, been corrected for the combined Lorentz–polarization factor

$$LP(\theta)=\frac{0{\cdot}538+0{\cdot}461\cos^2 2\theta}{\sin^2\theta\cos\theta}. \tag{3}$$

3. Experimental results and discussion

3.1. *X-ray diffraction patterns*

The cyclopalladated iodo-bridged complex obtained from {5-(1-nonyl)-{[4′(1-nonyloxy)2-phenylpyrimidine, HL_3, is a mesomorphic species whose phase diagram, as determined by optical microscopy and differential scanning calorimetry measurements, is C→105·1°C (S_A)→128·1°C (S_X)→202·5°C (I).

The diffraction patterns recorded at different temperatures between room temperature and the clearing temperature of about 200°C are shown in figure 2. As an example, figures 3 and 4 report the two dimensional pattern obtained at 100°C and 150°C, respectively, with the pin-hole flat camera. The results clearly show that the room temperature spectrum does not change up to approximately 75°C. In this temperature range the compound exhibits a solid phase, characterized by the presence of several peaks in the low angle region of the diffraction pattern. The lowest angle peak gives the maximum periodicity in the solid phase of 30·6 Å. A gradual modification of the diffraction pattern is observed starting from about 80°C until, at 105°C it finally takes the shape displayed in figure 2(*d*). This indicates that a broad phase transition takes place in this temperature range, as confirmed by DSC measurements. This modification of the diffraction pattern can be assigned to a solid→solid phase transition. The diffraction spectra of the two solid phases, C and C_1, differ in number and position of the peaks. In addition, the diffraction peaks for C_1 are sharper than for C while the contribution of the amorphous scattering to the total scattering (especially in the high angle region) seems to be greater from C, thus indicating a higher degree of crystallinity for the solid phase C_1. Only one peak is present in the high angle region of the C_1 spectrum, centred at 2θ of about 21°. The maximum periodicity in C_1 is approximately 29·5 Å and, in contrast to C, it is associated with the dominant peak in the low angle region. No higher order reflection of the main periodicity is present.

On increasing the temperature, the phase C_1 is stable until about 125°C where a phase transition to a disordered smectic mesophase takes place (see figure 2(*e*)). Since the interplanar distance corresponding to the low angle peak in the smectic phase is

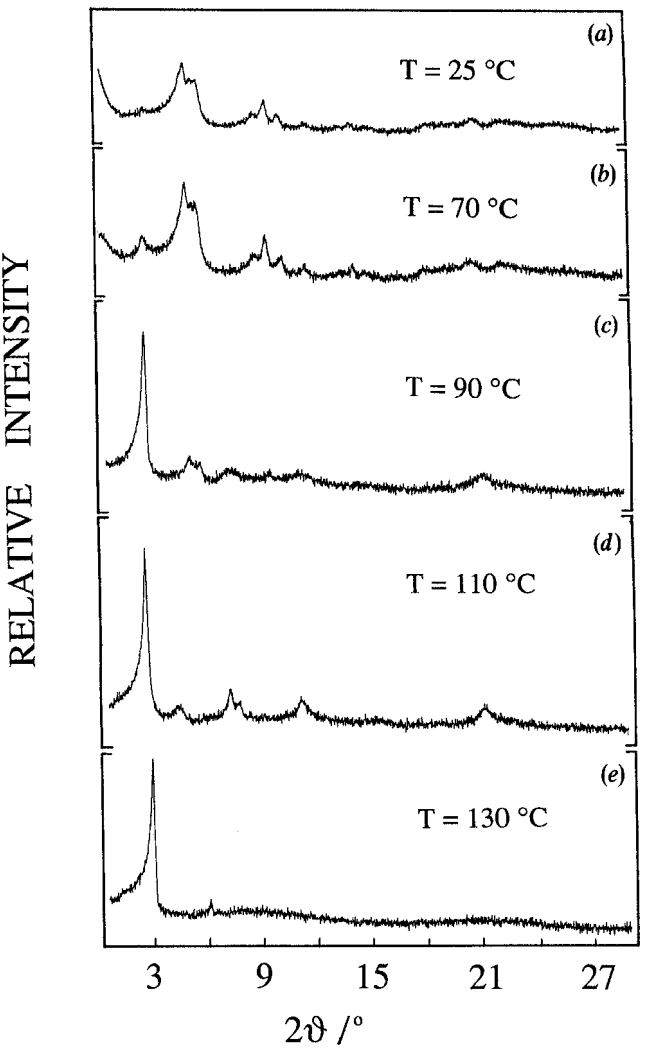

Figure 2. X-ray diffraction patterns at different temperatures for the cyclopalladated complex $[Pd(L_3)(\mu-I)]_2$ ($[Pd(L_3)(\mu-I)]_2$ = bis-{5-(1-nonyl)-2{[4′(1-nonyloxy)phenyl-2′-ato]}′ pyrimidine-N′, $C^{2'}$]-μ-iodo}dipalladium(II).

approximately the molecular length in the fully extended configuration (~30 Å), and taking into account the results of optical microscopy [2], the phase can be classified as smectic A. The broad diffuse halo in the high angle region is centred around 21° and corresponds to an average distance between neighbouring molecules within a smectic layer of about 4·2 Å. A further increase in the temperature does not modify the nature of the mesophase until 202·5°C, where the transition to the isotropic phase takes place.

The position of the low angle Bragg peak from the smectic phase depends sensitively on the temperature as shown in figure 5, where the temperature dependence of the maximum periodicity in the different mesophases is reported. The interplanar distance in the smectic phase decreases almost linearly from ~29·5 Å to ~28·0 Å in the range 125°C–180°C. This behaviour could be associated with the high mobility of the

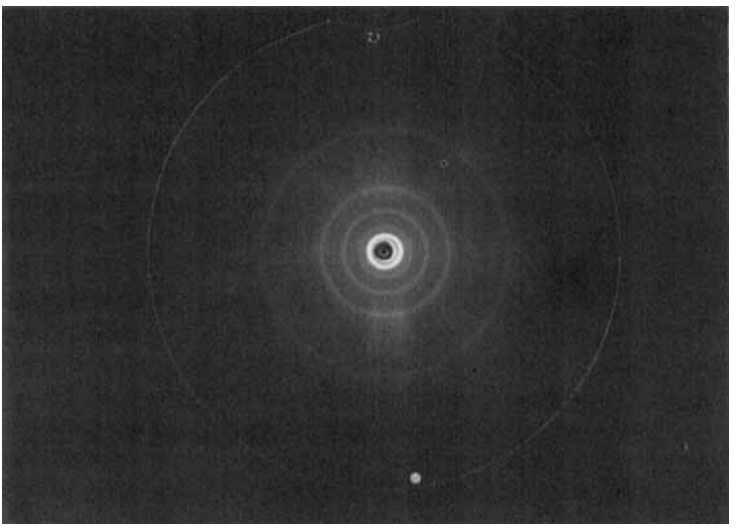

Figure 3. X-ray diffraction photograph at 100°C.

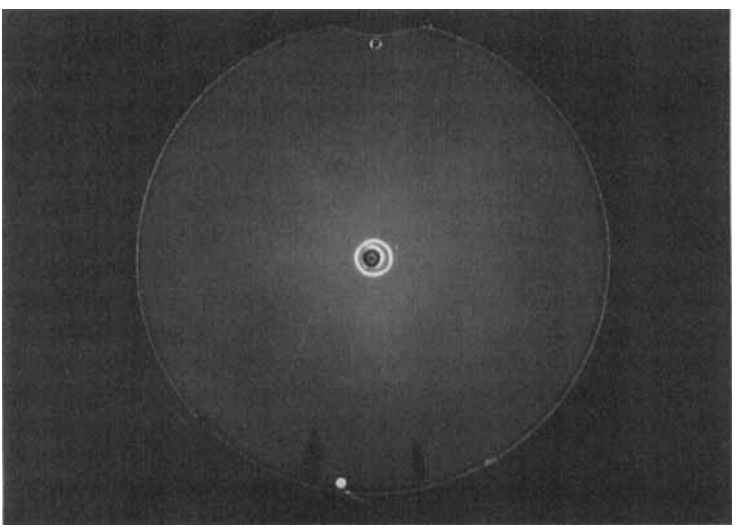

Figure 4. X-ray diffraction photograph in the smectic phase at 150°C.

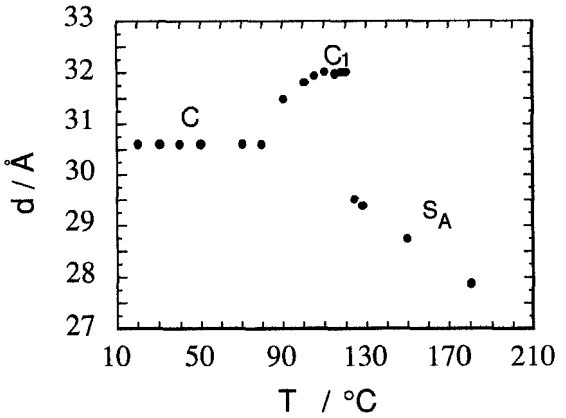

Figure 5. Maximum periodicity d in the different mesophases as a function of temperature: in the smectic phase d is the layer thickness.

aliphatic chains with increasing temperature. On the other hand, no remarkable temperature dependence is observed for the full width at half maximum of the Bragg peak.

A noticeable feature of the spectrum exhibited by the smectic phase is the presence of second order Bragg reflections from the smectic layers. This second order peak is present up to about 180°C. The presence of higher orders of reflection in the diffraction pattern means that the projection of the electron density profile along the normal to the smectic layers (director) cannot be described by the ideal model of a single sinusoidal modulation commonly employed for calamitic low molecular weight liquid crystals [12]. This reflects the influence of the peculiar features of the molecule, for example, the lateral–lateral fused structure and the high electron density contrast between the region of the cores and the aliphatic chains (because of the palladium and the iodine atoms). Therefore, in order to gain an insight into the differences between typical rod-like and these lateral–lateral fused mesogens, the electron density $\rho(z)$ along the director (z axis) of $[Pd(L_3)(\underline{\mu}\text{-I})]_2$ in the smectic phase has been determined. The calculation has been performed by means of Fourier inversion, following the procedure described in [13].

3.2. *Determination of the electron density profile along the director*

To perform such calculations, the intensities of the first and second order Bragg reflections must be determined. In our experiment it was not possible to obtain absolute intensities and the results are presented as the ratio $I_{(002)}/I_{(001)}$ of the intensity of the second order to the intensity of the first. The integrated intensities have been measured from the spectrum at 130°C and the result, after performing the corrections discussed in the experimental section, gives $I_{(002)}/I_{(001)}=0{\cdot}160$. Without loss of generality the origin of the z axis has been taken in the middle of the molecule, i.e. at the point corresponding to the position of the Pd atoms (see figure 1). With this choice $\rho(z)$ is symmetric, $\rho(-z)=\rho(z)$ and since it is a periodic function of the layer thickness d, it can be expressed as a Fourier series where only the cosine terms are relevant

$$\rho(z)=\rho_0+2\sum_{l=1}^{\infty}F_l\cos\left(2n\pi l\frac{z}{d}\right); \tag{4}$$

here ρ_0 is the average value of the electron density along the director and $F_l = F(0, 0, l)$ is the structure factor of the $\{00l\}$ reflection. Since ρ_0 is not measured but simply the fluctuations around it, here $\rho(z)$ represents only the fluctuations with $a_l = 2F_l$,

$$\rho(z) = \sum_l a_l \cos\left(2n\pi l \frac{z}{d}\right). \tag{5}$$

On the other hand ρ_0 can be easily evaluated by dividing the total number of electrons of the molecule by the dimension d of the unit cell (i.e. the layer thickness): $\rho_0 \sim 22 \pm 0{\cdot}5\,e^-/\text{Å}$.

In the present case the sum in equation (5) extends up to $l = 2$. The intensity $I(00l)$ of the lth order of reflection is related to a_l by

$$I(00l) = K|a_l|^2,$$

where K is a proportionality constant, so that $|a_2/a_1|^2 = I_{(002)}/I_{(001)}$. Once normalized to one the amplitude of the first order reflection ($|a_1| = 1$) the relation allows us to obtain $|a_2| = 0{\cdot}4$. Due to the centrosymmetric nature of the electron density distribution, the phase factor and the structure factor F_l must be either 0 or π, so that the coefficients a_1 are real but may be positive or negative. The phase problem then reduces to choosing the right combination of signs for the coefficients a_l ($l = 1, 2$). As an example ρ_{+-} symbolize the combination where a_1 is chosen to be positive while a_2 is negative. Four different distributions of the electron density correspond to the four combinations of signs of the coefficients a_1 and a_2. However, the one which is physically acceptable can

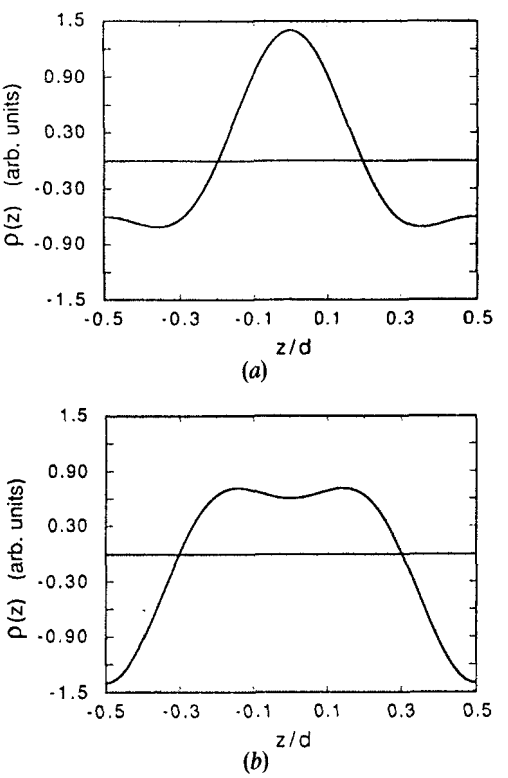

Figure 6. Electron density profiles along the normal to the smectic layers corresponding to different sign combinations of the a_n coefficients: (*a*) ρ_{++}, (*b*) ρ_{+-}.

be selected taking into account the molecular structure of the compound investigated (see figure 1). Thus, it is apparent that the central part of the molecule, which contains the 2-phenylpyrimidine cores and the Pd_2I_2 fragment, possess a much higher density with respect to the aliphatic chains. In particular, the maximum of $\rho(z)$ is expected to occur in the middle of the molecule, corresponding to the palladium and iodine atoms. Accordingly, we expect an electron density distribution with a sharp maximum centred at $z=0$. The electron density profiles resulting from the $(-,-)$ and $(-,+)$ combinations do not satisfy this condition and therefore can be rejected. The remaining combinations of signs $(+,+)$ and $(+,-)$ give rise to the two distributions shown in figures 6 (*a*) and (*b*), respectively. A choice of the physically acceptable solution can be made, as discussed in [13], with the use of Etherington's parameter r [14], defined by

$$r=\frac{\rho_0-\rho_{al}}{\rho_{core}-\rho_{al}}, \tag{6}$$

where ρ_{core} and ρ_{al} are the average density of, respectively, the rigid core and the aliphatic chains. The X-ray results give only relative values of the electron density, but the ratio r calculated from the experimentally determined function $\rho(z)$ may usefully be compared with values estimated for simple models. This parameter helps to appreciate which solution gives a proper electron density to the core compared with that of the aliphatic parts of the molecule.

From the model of the molecule in the fully extended configuration (see figure 1) we can calculate the electron density both of the mesogenic core and the aliphatic chains by dividing the total number of electrons in each of the two regions by their respective size. The size l_{core} of the rigid core of the molecule (containing the mesogenic cores and the ligand, palladium and iodine atoms) can be evaluated by considering the typical lengths of the different atomic groups. Thus, taking into account the structural results reported in [2], we obtain $l_{core}\sim 7$ Å and for the electron density $\rho_{core}\sim 51{\cdot}4\pm 0{\cdot}5\,e^-/Å$ (this is only a crude estimate because it neglects the translational fluctuations which spread out this electron density maximum). Similarly for the aliphatic parts, by taking the length of the aliphatic chains $l_{al}=(d-l_{core})/2$ with $l_{core}=7$ Å, we find $\rho_{al}\sim 12{\cdot}98\pm 0{\cdot}3\,e^-/Å$. With these values of ρ_{core} and ρ_{al} we find $r=0{\cdot}24\pm 0{\cdot}15$. On the other hand, the result of the calculation of r for each of the two possible solutions reported in figures 6 (*a*) and (*b*) gives, $r=0{\cdot}34$ and $0{\cdot}66$, respectively. Compared with the value of the model density $r=0{\cdot}24\pm 0{\cdot}15$ only the distribution in figure 6 (*a*) gives an acceptable value of r, therefore it can be considered to be the actual electron distribution. This result agrees with the physical consideration namely that it is extremely unlikely that the spreading of the central maximum associated with the translational fluctuations exceeds 50 per cent of the layer thickness d (as it does in figure 6 (*b*)). Moreover, it should be pointed out that these calculations agree for a maximum which spans about 10 Å. The $[Pd(L_3)(\mu\text{-}I)]_2$ molecule is nearly 30 Å long with a 7 Å rigid core. Therefore, the resulting electron density distribution (which accounts for translational fluctuations present to some extent) and the layer thickness (29·5 Å) both suggest that inside the smectic layers the aliphatic chains should be partially disordered.

With increasing temperature, the intensity of the second order reflection gradually reduces until at 180°C the peak disappears. In terms of electron distribution this means that the profile reported in figure 6 (*a*) is gradually modified until it takes the shape of a single sinusoidal modulation with a consequent spreading out of the central maximum. This behaviour can be understood on the basis of the higher translational fluctuations of the molecules and the greater mobility of the chains.

4. Conclusions

The X-ray diffraction investigation of the $[Pd(L_3)(\mu\text{-}I)]_2$ mesogen has shown a phase diagram consisting of C→105·1°C (C_1)→128·1°C (S_A)→202·5°C (I). The projection of the electron density profile along the normal to the smectic layers has been determined by measuring the intensities of the two orders of reflection. This gives information on the average localization of the aromatic cores of the molecules within the smectic layers (i.e. the degree of confinement of the high electron density rigid section of the smectic layer).

The peculiar features displayed by this lateral–lateral fused mesogen can be summarized as follows:

(i) the solid C_1 phase gives a polygonal texture like a smectic A phase so that, on the basis of optical microscopy, it was wrongly classified as S_A [2],

(ii) the subsequent mesophase, whose texture accounts for a S_A phase and previously classified as S_X [2], has been confirmed to be a true S_A phase.

(iii) to describe properly the electron density profile along the director a model which takes into account the high electron density area (i.e. the four aromatic rings and the Pd_2I_2 fragment) extending perpendicular to the director and relatively well-confined inside the smectic layers. This model of the electron density suggests an analogy with the situation encountered for some side-chain polymers possessing backbones with a large electron density [13, 15]. In both cases, in fact, some molecular moieties fluctuate less than observed for common mesogens, so that Debye–Waller factors take relatively low values.

This work was financed by the Italian Consiglio Nazionale delle Ricerche (CNR) and Ministero dell'Università e della Ricerca Scientifica e Tecnologica (MURST). We thank Johnson Matthey Research Centre, England, for a generous loan of $PdCl_2$.

References

[1] Giroud-Godquin, A. M., and Maitlis, P. M., 1991, *Angew. Chem. Int. Ed. Engl.*, **30**, 375.
[2] Ghedini, M., Pucci, D., De Munno, G., Viterbo, D., Neve, F., and Armentano, S., 1991, *Chem. Mater.*, **3**, 65.
[3] Hoshino, N., Hasegawa, H., and Matsunaga, Y., 1991, *Liq. Crystals*, **2**, 267.
[4] Ghedini, M., Morrone, S., De Munno, G., and Crispini, A., 1991, *J. Organomet. Chem.*, **415**, 281.
[5] Baena, M. J., Espinet, P., Ros, M. B., and Serrano, J. L., 1991, *Angew. Chem. Int. Ed. Engl.*, **30**, 711.
[6] Demus, D., 1989, *Liq. Crystals*, **5**, 75.
[7] Ghedini, M., Armentano, S., Bartolino, R., Torquati, G., and Rustichelli, F., 1987, *Solid St. Commun.*, **64**, 1191.
[8] Levelut, A. M., Ghedini, M., Bartolino, R., Nicoletta, F. P., and Rustichelli, F., 1989, *J. Phys., France*, **50**, 113.
[9] Barbera, G., Levelut, A. M., Marcos, M., Romero, P., and Serrano, J. L., 1991, *Liq. Crystals*, **10**, 119.
[10] Hosemann, R., and Bagchi, S. N., 1962, *Direct Analysis of Diffraction by Matter* (North-Holland).
[11] Kakudo, M., and Kasai, N., 1972, *X-ray Diffraction by Polymers* (Elsevier), Chap. 13, p. 358.
[12] De Gennes, P. G., 1974, *The Physics of Liquid Crystals* (Clarendon Press), Chap. 1, p. 13 and Chap. 7, p. 273.
[13] Davidson, P., Levelut, A. M., Achard, M. F., and Hardouin, F., 1989, *Liq. Crystals*, **4**, 561.
[14] Etherington, G., Langley, A. J., Leadbetter, A. J., and Wang, X. J., 1988, *Liq. Crystals*, **3**, 155.
[15] Gudkov, V. A., 1984, *Sov. Phys. Crystallogr.*, **29**, 316.